J. Fluid Mech. (2003), *vol.* 475, *pp.* 303–331.
DOI: 10.1017/S0022112002002823 Printed in the United Kingdom

Instability of quasi-geostrophic vortices in a two-layer ocean with a thin upper layer

By E. S. BENILOV

Department of Mathematics, University of Limerick, Ireland

(Received 8 March 2001 and in revised form 30 August 2002)

We examine the stability of a quasi-geostrophic vortex in a two-layer ocean with a thin upper layer on the f-plane. It is assumed that the vortex has a sign-definite swirl velocity and is localized in the upper layer, whereas the disturbance is present in both layers. The stability boundary-value problem admits three types of normal modes: fast (upper-layer-dominated) modes, responsible for equivalent-barotropic instability, and two slow baroclinic types (mixed- and lower-layer-dominated modes). Fast modes exist only for unrealistically small vortices (with a radius smaller than half of the deformation radius), and this paper is mainly focused on the slow modes. They are examined by expanding the stability boundary-value problem in powers of the ratio of the upper-layer depth to the lower-layer depth. It is demonstrated that the instability of slow modes, if any, is associated with critical levels, which are located at the periphery of the vortex. The complete (sufficient and necessary) stability criterion with respect to slow modes is derived: the vortex is stable if and only if the potential-vorticity gradient at the critical level and swirl velocity are of the same sign. Several vortex profiles are examined, and it is shown that vortices with a slowly decaying periphery are more unstable baroclinically and less barotropically than those with a fast-decaying periphery, with the Gaussian profile being the most stable overall. The asymptotic results are verified by numerical integration of the exact boundary-value problem, and interpreted using oceanic observations.

1. Introduction

Vortices play an important role in the dynamics of the ocean, yet their stability properties are still unclear. Apart from numerical studies of particular examples (e.g. Ikeda 1981; Helfrich & Send 1988; Carton & McWilliams 1989; Ripa 1992; Dewar & Killworth 1995), there is only one general result on the stability of baroclinic vortices – namely, that vortices with small Burger numbers are unstable (Killworth, Blundell & Dewar 1997; Benilov, Broutman & Kuznetsova 1998). Unfortunately, this is not useful, as the Burger numbers of many real-life oceanic vortices are of the order of unity (Olson 1991). Furthermore, models that yield instability do not resolve the main paradox associated with oceanic eddies: how can they exist for years if they are unstable? Thus, the only conclusion to be derived from the results of Killworth *et al.* (1997) and Benilov *et al.* (1998) is that stable vortices may not have small Burger number.

A more positive conclusion was obtained by Paldor & Nof (1990), who considered the particular case of lenses with zero potential vorticity (PV) in a two-layer ocean, and found them to be stable if they are sufficiently thin (it should be noted that most oceanic eddies are indeed thin).

However, the model of Paldor & Nof (1990) has an important shortcoming: the zero-PV vortex has constant angular velocity, which rules out critical levels. Unfortunately, this devalues the conclusion obtained, as critical levels are important for hydrodynamic stability and should be taken into account by any realistic model. Note also that the result of Paldor & Nof (1990) does not agree with the conclusion of Ripa (1992), who predicted instability for all vortices with constant angular velocity, regardless of their thicknesses.

The present paper examines the stability of vortices in a two-layer ocean with a thin upper layer. Attention is focused on quasi-geostrophic vortices (a study of ageostrophic vortices is in progress). Our approach is based on a single small parameter, the ratio of the depth of the upper layer to that of the lower layer. We consider arbitrary vortex profiles, and thus examine the effect of critical levels.

In § 2, we shall formulate the governing equations and demonstrate why the usual stability criterion (based on the monotonicity of potential vorticity) does not work for the problem at hand. In § 3, it will be shown that the problem admits three types of normal modes: *fast* (upper-layer-dominated) modes, responsible for equivalent-barotropic instability, and two types of *slow* baroclinic modes (mixed- and lower-layer-dominated modes). This paper is mostly devoted to the slow types: in §§ 4 and 5, we shall derive a stability criterion for these, and verify it by comparing with the numerical solution of the exact equations. In § 6, the results obtained will be interpreted using the observations of oceanic rings by Olson (1991).

2. Formulation

2.1. *Governing equations*

Consider a two-layer ocean with a rigid lid. Let the densities and depths of the layers be $\rho_{1,2}$ and $H_{1,2}$ (the subscript 1 marks the upper layer). We shall assume that the horizontal scale of the flow is of the order of the upper-layer deformation radius

$$L_d = \frac{1}{f}\sqrt{\frac{\rho_2 - \rho_1}{\rho_2} g H_1},$$

where g is the acceleration due to gravity and f is the Coriolis parameter. Using L_d and the characteristic velocity U of the flow in the upper layer, we introduce the following non-dimensional variables:

$$t = \frac{U t_*}{L_d}, \quad (x, y) = \frac{(x_*, y_*)}{L_d}, \quad \psi_{1,2} = \frac{\psi_{*1,2}}{L_d U},$$

where t is the time, (x, y) are the spatial coordinates, $\psi_{1,2}$ are the streamfunctions, and the asterisk marks the dimensional variables.

To describe vortices, we shall employ the standard quasigeostrophic equations on the f-plane,

$$\frac{\partial}{\partial t}\left(\nabla^2\psi_1 - \psi_1 + \psi_2\right) + J(\psi_1, \nabla^2\psi_1 + \psi_2) = 0, \tag{2.1}$$

$$\frac{\partial}{\partial t}(\nabla^2\psi_2 - \varepsilon\psi_2 + \varepsilon\psi_1) + J(\psi_2, \nabla^2\psi_2 + \varepsilon\psi_1) = 0, \tag{2.2}$$

where $J(\psi_1, \psi_2)$ is the Jacobian operator and ε is the depth ratio,

$$\varepsilon = \frac{H_1}{H_2}.$$

We are concerned with the stability of radially symmetric vortices with respect to

small disturbances,

$$\psi_{1,2} = \Psi_{1,2}(r) + \psi'_{1,2}(r, \theta, t), \tag{2.3}$$

where the capital-letter variables describe the vortex, the primed variables describe the disturbance, and (r, θ) are polar coordinates. Then we linearize the governing equations against the background of the vortex solution, i.e. substitute (2.3) into (2.1)–(2.2) and omit the nonlinear terms,

$$\frac{\partial}{\partial t}(\nabla^2\psi'_1 - \psi'_1 + \psi'_2) + J(\Psi_1, \nabla^2\psi'_1 + \psi'_2) + J(\psi'_1, \nabla^2\Psi_1 + \Psi_2) = 0,$$

$$\frac{\partial}{\partial t}(\nabla^2\psi'_2 - \varepsilon\psi'_2 + \varepsilon\psi'_1) + J(\Psi_2, \nabla^2\psi'_1 + \varepsilon\psi'_1) + J(\psi'_2, \nabla^2\Psi_1 + \varepsilon\Psi_1) = 0.$$

We shall consider harmonic disturbances,

$$\psi'_{1,2}(r, \theta, t) = \mathrm{Re}[\psi_{1,2}(r)\, \mathrm{e}^{\mathrm{i}k(\theta - ct)}],$$

where k and c are the azimuthal wavenumber and angular phase speed, respectively. Then, the governing equations become

$$c\left[\frac{1}{r}\frac{\mathrm{d}}{\mathrm{d}r}\left(r\frac{\mathrm{d}\psi_1}{\mathrm{d}r}\right) - \frac{k^2}{r^2}\psi_1 - \psi_1 + \psi_2\right] - \frac{1}{r}V_1\left[\frac{1}{r}\frac{\mathrm{d}}{\mathrm{d}r}\left(r\frac{\mathrm{d}\psi_1}{\mathrm{d}r}\right) - \frac{k^2}{r^2}\psi_1 + \psi_2\right]$$
$$+\frac{1}{r}\psi_1\left\{\frac{\mathrm{d}}{\mathrm{d}r}\left[\frac{1}{r}\frac{\mathrm{d}}{\mathrm{d}r}(rV_1)\right] + V_2\right\} = 0, \tag{2.4}$$

$$c\left[\frac{1}{r}\frac{\mathrm{d}}{\mathrm{d}r}\left(r\frac{\mathrm{d}\psi_2}{\mathrm{d}r}\right) - \frac{k^2}{r^2}\psi_2 - \varepsilon\psi_2 + \varepsilon\psi_1\right] - \frac{1}{r}V_2\left[\frac{1}{r}\frac{\mathrm{d}}{\mathrm{d}r}\left(r\frac{\mathrm{d}\psi_2}{\mathrm{d}r}\right) - \frac{k^2}{r^2}\psi_2 + \varepsilon\psi_1\right]$$
$$+\frac{1}{r}\psi_2\left\{\frac{\mathrm{d}}{\mathrm{d}r}\left[\frac{1}{r}\frac{\mathrm{d}}{\mathrm{d}r}(rV_2)\right] + \varepsilon V_1\right\} = 0 \tag{2.5}$$

where

$$V_{1,2} = \frac{\mathrm{d}\Psi_{1,2}}{\mathrm{d}r}$$

are the swirl velocities in the layers.

Equations (2.4)–(2.5) should be supplemented by the usual boundary conditions,

$$\psi_{1,2}(0) = \psi_{1,2}(\infty) = 0. \tag{2.6}$$

Equations (2.4)–(2.6) form an eigenvalue problem, where c is the eigenvalue. If $\mathrm{Im}\, c > 0$, the vortex is unstable.

2.2. *What do we want to achieve?*

As usual, a stability criterion based on the monotonicity of potential vorticity (PV) can be derived for (2.4)–(2.5) – see, for example, Dritschel (1988). In this subsection, we shall demonstrate that this criterion does not work for the problem at hand, and then outline how it can be improved.

First, rearrange equations (2.4)–(2.5) as follows:

$$\frac{\mathrm{d}}{\mathrm{d}r}\left(r\frac{\mathrm{d}\psi_1}{\mathrm{d}r}\right) - \left(\frac{k^2}{r} + r - \frac{\mathrm{d}Q_1/\mathrm{d}r}{V_1/r - c}\right)\psi_1 = -r\psi_2, \tag{2.7}$$

$$\frac{\mathrm{d}}{\mathrm{d}r}\left(r\frac{\mathrm{d}\psi_2}{\mathrm{d}r}\right) - \left(\frac{k^2}{r} + \varepsilon r - \frac{\mathrm{d}Q_2/\mathrm{d}r}{V_1/r - c}\right)\psi_2 = -\varepsilon r\psi_1, \tag{2.8}$$

where the PV gradients in the upper/lower layers are given by

$$\frac{\mathrm{d}Q_1}{\mathrm{d}r} = \frac{\mathrm{d}}{\mathrm{d}r}\left[\frac{1}{r}\frac{\mathrm{d}}{\mathrm{d}r}(rV_1)\right] - V_1 + V_2, \quad \frac{\mathrm{d}Q_2}{\mathrm{d}r} = \frac{\mathrm{d}}{\mathrm{d}r}\left[\frac{1}{r}\frac{\mathrm{d}}{\mathrm{d}r}(rV_2)\right] - V_2 + V_1.$$

Next, consider the following combination of equations (2.7) and (2.8):

$$\mathrm{Im}\int_0^\infty \left[(2.7)\times\psi_1^* + \frac{1}{\varepsilon}(2.8)\times\psi_2^*\right]\mathrm{d}r,$$

where the asterisk denotes complex conjugate. Integrating by parts and using boundary condition (2.6), we obtain

$$(\mathrm{Im}\, c)\int_0^\infty \left[\frac{\mathrm{d}Q_1/\mathrm{d}r|\psi_1|^2}{(V_1/r - \mathrm{Re}\, c)^2 + (\mathrm{Im}\, c)^2} + \frac{1}{\varepsilon}\frac{\mathrm{d}Q_2/\mathrm{d}r|\psi_2|^2}{(V_2/r - \mathrm{Re}\, c)^2 + (\mathrm{Im}\, c)^2}\right]\mathrm{d}r = 0. \tag{2.9}$$

Now, if $\mathrm{d}Q_1/\mathrm{d}r$ and $\mathrm{d}Q_2/\mathrm{d}r$ do not change sign and are of the same sign,

$$\frac{\mathrm{d}Q_1}{\mathrm{d}r}\frac{\mathrm{d}Q_2}{\mathrm{d}r} \geqslant 0 \quad \text{for all } r \in (0,\infty), \tag{2.10}$$

the vortex is stable ($\mathrm{Im}\, c = 0$), which provides a necessary criterion of instability.

It turns out, however, that condition (2.10) does not hold for any realistic oceanic vortex; given that their velocity decays rapidly with depth, we can assume that $V_2 = 0$, and the PV gradients become

$$\frac{\mathrm{d}Q_1}{\mathrm{d}r} = \frac{\mathrm{d}}{\mathrm{d}r}\left[\frac{1}{r}\frac{\mathrm{d}}{\mathrm{d}r}(rV_1)\right] - V_1, \quad \frac{\mathrm{d}Q_2}{\mathrm{d}r} = V_1. \tag{2.11}$$

Next, assume that the vortex is smooth at the origin and decays at infinity, which implies

$$V_1(0) = 0, \quad V_1(\infty) = 0.$$

Then one can see that $V_1(r)$ has at least one maximum, where it is positive, or at least one minimum, where it is negative. Assuming, say, the former, we conclude that there is a point $r = r_{\max}$ such that

$$(V_1)_{r=r_{\max}} > 0, \quad \left(\frac{\mathrm{d}V_1}{\mathrm{d}r}\right)_{r=r_{\max}} = 0, \quad \left(\frac{\mathrm{d}^2V_1}{\mathrm{d}r^2}\right)_{r=r_{\max}} \leqslant 0.$$

Then, (2.11) yields

$$\left(\frac{\mathrm{d}Q_1}{\mathrm{d}r}\right)_{r=r_{\max}} = \left(\frac{\mathrm{d}^2V_1}{\mathrm{d}r^2} + \frac{1}{r}\frac{\mathrm{d}V_1}{\mathrm{d}r} - \frac{1}{r^2}V_1 - V_1\right)_{r=r_{\max}} < 0,$$

$$\left(\frac{\mathrm{d}Q_2}{\mathrm{d}r}\right)_{r=r_{\max}} = (V_1)_{r=r_{\max}} > 0.$$

Thus, at $r = r_{\max}$, the signs of the PV gradients are opposite, which makes all vortices potentially unstable and renders the stability criterion (2.10) useless.

It should be noted, however, that (2.10) has been derived without any knowledge of the properties of the eigenfunctions $\psi_{1,2}$. In order to illustrate how they could affect a stability criterion, assume, for the sake of argument, that $|\psi_1| \gg |\psi_2|$. In this case, (2.9) results in a much tighter stability criterion, namely, that $\mathrm{d}Q_1/\mathrm{d}r$ be a sign-definite function of r.

In what follows, the boundary-value problem (2.4)–(2.6) with $V_2 = 0$ will be examined asymptotically on the basis of the assumption that the upper layer is

thin, i.e.

$$\varepsilon = \frac{H_1}{H_2} \ll 1.$$

Using asymptotic estimates of $\psi_{1,2}$, we shall tighten up the usual instability criterion, and make it necessary and sufficient.

3. Preliminary asymptotic analysis: three types of modes

Assume that the vortex is localized in the upper layer of the ocean, i.e.

$$V_2 = 0.$$

Then (2.4)–(2.5) become

$$c\left[\frac{1}{r}\frac{\mathrm{d}}{\mathrm{d}r}\left(r\frac{\mathrm{d}\psi_1}{\mathrm{d}r}\right) - \frac{k^2}{r^2}\psi_1 - \psi_1 + \psi_2\right] - \frac{1}{r}V_1\left[\frac{1}{r}\frac{\mathrm{d}}{\mathrm{d}r}\left(r\frac{\mathrm{d}\psi_1}{\mathrm{d}r}\right) - \frac{k^2}{r^2}\psi_1 + \psi_2\right] + \frac{1}{r}\psi_1\frac{\mathrm{d}}{\mathrm{d}r}\left[\frac{1}{r}\frac{\mathrm{d}}{\mathrm{d}r}(rV_1)\right] = 0, \quad (3.1)$$

$$c\left[\frac{1}{r}\frac{\mathrm{d}}{\mathrm{d}r}\left(r\frac{\mathrm{d}\psi_2}{\mathrm{d}r}\right) - \frac{k^2}{r^2}\psi_2 - \varepsilon\psi_2 + \varepsilon\psi_1\right] + \varepsilon\frac{1}{r}V_1\psi_2 = 0. \quad (3.2)$$

We shall also assume that the upper-layer velocity is a smooth, fast-decaying function:

$$V_1 = o(r^{-4}) \quad \text{as} \quad r \to \infty,$$

and that the corresponding angular velocity is monotonic:

$$\frac{\mathrm{d}}{\mathrm{d}r}\left(\frac{1}{r}V_1\right) \neq 0$$

(the latter condition guarantees that each normal mode has no more than one critical level, i.e. a point where $V_1/r = \mathrm{Re}\, c$). We shall also assume that $V_1(r)$ is a sign-definite function, which is usually the case in the ocean.

We shall seek the solution to the boundary-value problem (3.1)–(3.2), (2.6) in the form

$$c = c^{(0)} + \varepsilon c^{(1)} + \varepsilon^2 c^{(2)} + \cdots, \quad \psi_{1,2} = \psi_{1,2}^{(0)} + \varepsilon\psi_{1,2}^{(1)} + \cdots .$$

It can be readily seen that, if $\omega^{(0)} \neq 0$ and $\psi_2^{(0)} \neq 0$, the leading order of the lower-layer equation

$$c^{(0)}\left[\frac{1}{r}\frac{\mathrm{d}}{\mathrm{d}r}\left(r\frac{\mathrm{d}\psi_2^{(0)}}{\mathrm{d}r}\right) - \frac{k^2}{r^2}\psi_2^{(0)}\right] = 0,$$

has no bounded solutions. Thus, either $\psi_2^{(0)}$ or $c^{(0)}$ or both have to be zero, depending on which we shall consider three types of modes:

(i) If

$$\psi_2^{(0)} = 0, \quad c^{(0)} \neq 0,$$

the upper-layer equation (3.1), to the leading order, decouples from its lower-layer counterpart:

$$c^{(0)}\left[\frac{1}{r}\frac{\mathrm{d}}{\mathrm{d}r}\left(r\frac{\mathrm{d}\psi_1^{(0)}}{\mathrm{d}r}\right) - \frac{k^2}{r^2}\psi_1^{(0)} - \psi_1^{(0)}\right] - \frac{1}{r}\left\{V_1\left[\frac{1}{r}\frac{\mathrm{d}}{\mathrm{d}r}\left(r\frac{\mathrm{d}\psi_1^{(0)}}{\mathrm{d}r}\right) - \frac{k^2}{r^2}\psi_1^{(0)}\right] - \psi_1^{(0)}\frac{\mathrm{d}}{\mathrm{d}r}\left[\frac{1}{r}\frac{\mathrm{d}}{\mathrm{d}r}(rV_1)\right]\right\} = 0. \quad (3.3)$$

It describes the usual equivalent-barotropic motion, and its solutions will be referred to as *upper-layer-dominated* (*ULD*) *modes*.

(ii) If

$$\psi_2^{(0)} \neq 0, \quad c^{(0)} = 0,$$

equations (3.1)–(3.2) become

$$-V_1\left[\frac{1}{r}\frac{\mathrm{d}}{\mathrm{d}r}\left(r\frac{\mathrm{d}\psi_1^{(0)}}{\mathrm{d}r}\right) - \frac{k^2}{r^2}\psi_1^{(0)} - \psi_1^{(0)} + \psi_2^{(0)}\right] + \left\{\frac{\mathrm{d}}{\mathrm{d}r}\left[\frac{1}{r}\frac{\mathrm{d}}{\mathrm{d}r}(rV_1)\right] - V_1\right\}\psi_1^{(0)} = 0, \quad (3.4)$$

$$c^{(1)}\left[\frac{1}{r}\frac{\mathrm{d}}{\mathrm{d}r}\left(r\frac{\mathrm{d}\psi_2^{(0)}}{\mathrm{d}r}\right) - \frac{k^2}{r^2}\psi_2^{(0)}\right] + \frac{1}{r}\psi_2^{(0)}V_1 = 0. \quad (3.5)$$

In this case, $c^{(1)}$ is fully determined by the lower-layer equation, which decouples from its upper-layer counterpart. It describes oscillations in a layer with non-even upper boundary, and its solutions will be referred to as *lower-layer-dominated* (*LLD*) *modes* (although ψ_1 and ψ_2, in this case, are of the same order, the larger thickness of the lower layer makes it dominant). They exist due to the curvature of the interface and, dynamically, are not sensitive to the flow in the upper layer (just as waves trapped by bottom irregularities are not sensitive to what happens below the bottom of the ocean). The upper-layer equation (3.4), in turn, describes a disturbance forced by the oscillations in the lower layer.

(iii) If

$$\psi_2^{(0)} = 0, \quad c^{(0)} = 0,$$

the eigenvalue c, to the leading order, drops out from the upper-layer equation:

$$V_1\left[\frac{1}{r}\frac{\mathrm{d}}{\mathrm{d}r}\left(r\frac{\mathrm{d}\psi_1^{(0)}}{\mathrm{d}r}\right) - \frac{k^2}{r^2}\psi_1^{(0)}\right] - \psi_1^{(0)}\frac{\mathrm{d}}{\mathrm{d}r}\left[\frac{1}{r}\frac{\mathrm{d}}{\mathrm{d}r}(rV_1)\right] = 0. \quad (3.6)$$

$c^{(1)}$ is to be determined from the next-order equations:

$$c^{(1)}\left[\frac{1}{r}\frac{\mathrm{d}}{\mathrm{d}r}\left(r\frac{\mathrm{d}\psi_1^{(0)}}{\mathrm{d}r}\right) - \frac{k^2}{r^2}\psi_1^{(0)} - \psi_1^{(0)}\right] - \frac{1}{r}\left\{V_1\left[\frac{1}{r}\frac{\mathrm{d}}{\mathrm{d}r}\left(r\frac{\mathrm{d}\psi_1^{(1)}}{\mathrm{d}r}\right) - \frac{k^2}{r^2}\psi_1^{(1)} + \psi_2^{(1)}\right] - \psi_1^{(1)}\frac{\mathrm{d}}{\mathrm{d}r}\left[\frac{1}{r}\frac{\mathrm{d}}{\mathrm{d}r}(rV_1)\right]\right\} = 0, \quad (3.7)$$

$$c^{(1)}\left[\frac{1}{r}\frac{\mathrm{d}}{\mathrm{d}r}\left(r\frac{\mathrm{d}\psi_2^{(1)}}{\mathrm{d}r}\right) - \frac{1}{r^2}\psi_2^{(1)} + \psi_1^{(0)}\right] + \frac{1}{r}\psi_2^{(1)}V_1 = 0. \quad (3.8)$$

Importantly, (3.7)–(3.8) include both leading-order eigenfunctions, $\psi_1^{(0)}$ and $\psi_2^{(1)}$, hence the corresponding solutions will be referred to as *mixed modes*.

Observe that the last two types of modes are both slow ($c \approx \varepsilon c^{(1)} \ll 1$) and are responsible for baroclinic instability, whereas fast ULD modes ($c \approx c^{(0)} \sim 1$) are responsible for equivalent-barotropic instability. It can be demonstrated (see below) that the latter type of instability is not relevant to the mesoscale oceanic vortices (which we are mostly interested in); therefore this paper is almost entirely devoted to slow modes. Their properties will be examined in the next two sections.

4. Mixed modes

In this section, we shall examine mixed modes. Surprisingly, the first two orders of the asymptotic expansion will turn out to be neutrally stable. In order to find the growth rate, higher orders will have to be explored.

4.1. *Zeroth-order results: a restriction to the first azimuthal wavenumber*

The zeroth-order equation (3.6) should be supplemented by the boundary condition

$$\psi_1^{(0)}(0) = \psi_1^{(0)}(\infty) = 0. \tag{4.1}$$

Observe that the eigenvalue $c^{(1)}$ appears in neither the equation nor the boundary condition, which makes it unlikely that (3.6), (4.1) has a solution.

The boundary-value problem (3.6), (4.1) *has a solution only for the first azimuthal wavenumber* $k = 1$, *in which case* $\psi_1^{(0)} = V_1$.

In order to prove the above statement, rewrite (3.6) in terms of a new variable χ:

$$\psi_1^{(0)} = V_1\chi. \tag{4.2}$$

Substituting (4.2) into (3.6), we obtain

$$\frac{\mathrm{d}}{\mathrm{d}r}\left(rV_1^2\frac{\mathrm{d}\chi}{\mathrm{d}r}\right) - \frac{k^2-1}{r}V_1^2\chi = 0.$$

Now, multiply this equation by χ^* and integrate over $0 < r < \infty$. Integrating by parts, we obtain

$$\int_0^\infty V_1^2\left(r\left|\frac{\mathrm{d}\chi}{\mathrm{d}r}\right|^2 + \frac{k^2-1}{r}|\chi|^2\right)\mathrm{d}r = 0.$$

Clearly, if $k \geqslant 2$, then

$$\frac{\mathrm{d}\chi}{\mathrm{d}r} = 0, \quad \chi = 0 \quad \text{at all points where } V_1 \neq 0,$$

which makes χ zero everywhere (if a solution and its derivative of a second-order ODE with continuous coefficients are both zero at the same point, this solution is zero identically). If, however, $k = 1$, the solution evidently exists: $\chi = \text{const}$. Putting const $= 1$ and recalling (4.2), we obtain

$$\psi_1^{(0)} = V_1,$$

as required. (This solution often comes up in stability problems; it corresponds to an infinitesimal shift of the vortex as a solid.)

Thus, we need to examine mixed modes for only the first azimuthal wavenumber, $k = 1$.

4.2. *First-order results: neutral stability?*

For $k = 1$ and $\psi_1^{(0)} = V_1$, the first-order equations (3.7)–(3.8) become

$$c^{(1)}\left[\frac{1}{r}\frac{\mathrm{d}}{\mathrm{d}r}\left(r\frac{\mathrm{d}V_1}{\mathrm{d}r}\right) - \frac{1}{r^2}V_1 - V_1\right] - \frac{1}{r}\left\{V_1\left[\frac{1}{r}\frac{\mathrm{d}}{\mathrm{d}r}\left(r\frac{\mathrm{d}\psi_1^{(1)}}{\mathrm{d}r}\right) - \frac{1}{r^2}\psi_1^{(1)} + \psi_2^{(1)}\right]\right.$$
$$\left. - \psi_1^{(1)}\frac{\mathrm{d}}{\mathrm{d}r}\left[\frac{1}{r}\frac{\mathrm{d}}{\mathrm{d}r}(rV_1)\right]\right\} = 0, \tag{4.3}$$

$$c^{(1)}\left[\frac{1}{r}\frac{\mathrm{d}}{\mathrm{d}r}\left(r\frac{\mathrm{d}\psi_2^{(1)}}{\mathrm{d}r}\right)-\frac{1}{r^2}\psi_2^{(1)}+V_1\right]+\frac{1}{r}\psi_2^{(1)}V_1=0. \tag{4.4}$$

It is convenient to eliminate $\psi_1^{(1)}$, which can be done by multiplying (4.3) by r^2 and integrating over $0<r<\infty$. Integrating by parts, we obtain

$$\int_0^\infty rV_1\psi_2^{(1)}\mathrm{d}r+c^{(1)}\int_0^\infty r^2V_1\mathrm{d}r=0. \tag{4.5}$$

We shall also impose the usual boundary conditions

$$\psi_2^{(1)}(0)=\psi_2^{(1)}(\infty)=0. \tag{4.6}$$

Equations (4.4)–(4.6) form an eigenvalue problem for $\psi_2^{(1)}$ and $c^{(1)}$. In principle, the integral condition (4.5) can be transformed into a usual type of (differential) boundary condition (see Appendix A), which is more convenient numerically.

The main result of this subsection is as follows (its proof can be found in Appendix B):

All eigenvalues of (4.4)–(4.6) *are real.*

Thus, to the leading order, all disturbances are neutrally stable.

Another important result can be obtained as a by-product of the above theorem (it follows from identity (B 8) of Appendix B):

If $V_1(r)$ *is sign definite, the eigenvalues of* (4.4)–(4.6) *are of the same sign as* V_1.

Finally, we shall briefly discuss the existence of solutions to the boundary-value problem (4.4)–(4.6). It can be argued that (4.4)–(4.6) have an infinite sequence of eigenvalues converging to zero. The argument is based on the fact that the limit $c^{(1)}\to 0$ coincides with the WKB limit, using which one can calculate $c^{(1)}$ explicitly. This calculation has been performed for the particular case of 'vortices with finite support',

$$V_1=0 \quad \text{if} \quad r\geqslant R,$$

with the additional assumption that

$$V_1\to \text{const}(R-r)^n \quad \text{as} \quad r\to R-0,$$

where $n\geqslant 1$. (The WKB method, of course, is applicable to any vortex profile, but, unfortunately, the technical details depend on the specific form of the asymptotics of $V_1(r)$ as $r\to\infty$, and the issue of existence cannot be resolved in the general case.) It is also worth mentioning that, in addition to vortices with finite support, several cases of $V_1(r)$ were examined numerically (see below), and in all those cases the first-order boundary-value problem, as expected, did have a sequence of real eigenvalues converging to zero.

4.3. *Higher-order approximations: critical levels*

Observe that the problem at hand admits critical levels. Assuming for simplicity that $V_1(r)$ is a sign-definite function (which is the case oceanographically), one can see that

(i) the zeroth-order angular phase speed of the disturbance is real and has the same sign as V_1/r,

(ii) the absolute value of the phase speed is smaller than the maximum absolute value of V_1/r (the former is $O(\varepsilon)$, while the latter is $O(1)$).

Hence, the angular phase speed, $\mathrm{Re}\, c$, of the disturbance lies within the range

$$\left[\min\left\{\frac{1}{r}V_1(r)\right\}, \max\left\{\frac{1}{r}V_1(r)\right\}\right],$$

and a critical level (critical radius) r_c exists, such that

$$\frac{1}{r_c}V_1(r_c) = \mathrm{Re}\, c.$$

It is well-known that critical levels of neutrally stable modes cause singularities. However, our asymptotic equations have regular coefficients, and we have to conclude that the leading-order approximation describes critical levels incorrectly.

In order to understand why this should be so, consider the exact equation (2.7) and observe that, for neutrally stable eigenvalues, the last term in brackets is singular at $r = r_c$. To the leading order, however, this singularity cancels out. Indeed, as $c = O(\varepsilon)$ and $V_1/r = O(1)$, we should neglect the former in comparison with the latter. As a result, the critical level moves to infinity, where the numerator of the singular term vanishes as well, and the singularity cancels out.

The fact that the critical layer has not been 'grasped' by the first two orders of our expansion indicates that its effect is weak: first, the critical layer is narrow and, secondly, is located at the periphery of the vortex, where the eigenfunction is decaying. It can be safely assumed that its contribution to the eigenvalue is small – but no matter how small, it can be imaginary and, hence, cause instability. Mathematically, this means that one of the higher-order corrections to c can be imaginary.

Unfortunately, the straightforward approach to higher-order calculations gives rise to cumbersome algebra. Moreover, $\mathrm{Im}\, c$ may scale with a fractional power of ε, or even be exponentially small, which would make the perturbation expansion extremely awkward. Normally, this would mean that the problem at hand is intractable by analytical means. It turns out, however, that this particular problem allows a 'short-cut' to $\mathrm{Im}\, c$, which bypasses the calculation of the higher-order eigenfunction.

We start from the exact identity (2.9), put $V_2 = 0$, and simplify its second term by assuming

$$\psi_2 \approx \varepsilon\psi_2^{(1)}, \quad \mathrm{Re}\, c \approx \varepsilon c^{(1)} \tag{4.7}$$

and

$$|\mathrm{Im}\, c| \ll |\mathrm{Re}\, c| \tag{4.8}$$

(the latter inequality follows from the fact that, to the leading order, c has turned out to be real). After simple algebra, we obtain

$$\int_0^\infty \frac{\mathrm{Im}\, c}{(\mathrm{Re}\, c - V_1/r)^2 + (\mathrm{Im}\, c)^2}\frac{\mathrm{d}Q_1}{\mathrm{d}r}|\psi_1|^2\,\mathrm{d}r + (\mathrm{Im}\, c)\int_0^\infty V_1\left(\frac{\psi_2^{(1)}}{c^{(1)}}\right)^2\mathrm{d}r \approx 0. \tag{4.9}$$

Observe that a naive substitution of (4.7)–(4.8) into the first term of (4.9) would cause a divergence at the critical level $r = r_c$.

In the remainder of this section, we shall rearrange and simplify the first term of (4.9). The key point is the observation that the vortex can be subdivided into a *core* and *periphery*:

$$\frac{1}{r}V_1 \gg \mathrm{Re}\, c \quad \text{if} \quad r < r_b,$$

and

$$\frac{1}{r}V_1 \lesssim \mathrm{Re}\, c \quad \text{if} \quad r > r_b,$$

where r_b is an approximate boundary separating the two regions. Accordingly,

$$\int_0^\infty \frac{\mathrm{d}Q_1}{\mathrm{d}r}\,|\psi_1|^2\,\frac{\mathrm{Im}\, c}{(V_1/r - \mathrm{Re}\, c)^2 + (\mathrm{Im}\, c)^2}\mathrm{d}r = I_{core} + I_{peri}.$$

First, we shall consider

$$I_{core} = \int_0^{r_b} \frac{\mathrm{d}Q_1}{\mathrm{d}r}\,|\psi_1|^2\,\frac{\mathrm{Im}\, c}{(V_1/r - \mathrm{Re}\, c)^2 + (\mathrm{Im}\, c)^2}\mathrm{d}r.$$

The integrand of I_{core} can be simplified by omitting the small $\mathrm{Re}\, c$ and $\mathrm{Im}\, c$ in the denominator. We can also replace ψ_1 with its leading-order approximation: $\psi_1 \approx \psi_1^{(0)} = V_1$ and obtain

$$I_{core} \approx (\mathrm{Im}\, c)\int_0^{r_b} r^2\frac{\mathrm{d}Q_1}{\mathrm{d}r}\mathrm{d}r.$$

As $\mathrm{d}Q_1/\mathrm{d}r$ becomes small as $r \to \infty$, we can move the upper limit of I_{core} to infinity. Then, replacing $\mathrm{d}Q_1/\mathrm{d}r$ with its definition (2.11) and integrating by parts, we obtain

$$I_{core} \approx -(\mathrm{Im}\, c)\int_0^\infty r^2 V_1\,\mathrm{d}r.$$

The periphery term,

$$I_{peri} = \int_{r_b}^\infty \frac{\mathrm{d}Q_1}{\mathrm{d}r}\,|\psi_1|^2\,\frac{\mathrm{Im}\, c}{(V_1/r - \mathrm{Re}\, c)^2 + (\mathrm{Im}\, c)^2}\mathrm{d}r,$$

is mainly composed of the contribution of the critical layer (where the denominator of the integrand is small). This region is narrow, and the change of $V_1(r)$ over its width is small; hence, we can expand V_1/r, $\mathrm{d}Q_1/\mathrm{d}r$, and $|\psi_1|^2$ about $r = r_c$, for example,

$$\frac{1}{r}V_1(r) = \frac{1}{r_c}V_1(r_c) + \left[\frac{\mathrm{d}}{\mathrm{d}r}\left(\frac{1}{r}V_1\right)\right]_{r=r_c}(r - r_c) + \cdots .$$

We shall also move the lower limit of integration to $-\infty$ (since the integrand decays rapidly away from the critical level, this does not make much difference). Thus,

$$I_{peri} \approx (\mathrm{Im}\, c)\left(\frac{\mathrm{d}Q_1}{\mathrm{d}r}\,|\psi_1|^2\right)_{r=r_c}\int_{-\infty}^\infty \frac{\mathrm{d}r}{\{[(\mathrm{d}/\mathrm{d}r)(V_1/r)]_{r=r_c}(r - r_c)\}^2 + (\mathrm{Im}\, c)^2}.$$

Now, the integral can be evaluated:

$$I_{peri} \approx \pi\left[\frac{\mathrm{d}Q_1/\mathrm{d}r\,|\psi_1|^2}{|(\mathrm{d}/\mathrm{d}r)(V_1/r)|}\right]_{r=r_c}\mathrm{sign}(\mathrm{Im}\, c).$$

Substituting I_{core} and I_{peri} into (4.9), we obtain

$$\pi\left[\frac{(\mathrm{d}Q_1/\mathrm{d}r)\,|\psi_1|^2}{|(\mathrm{d}/\mathrm{d}r)(V_1/r)|}\right]_{r=r_c}\mathrm{sign}(\mathrm{Im}\, c) - (\mathrm{Im}\, c)\int_0^\infty r^2 V_1\,\mathrm{d}r + (\mathrm{Im}\, c)\int_0^\infty V_1\left(\frac{\psi_2^{(1)}}{c^{(1)}}\right)^2\mathrm{d}r \approx 0.$$

This equality can be rearranged using condition (4.5):

$$|\mathrm{Im}\, c| \int_0^\infty V_1(\psi_2^{(1)} + c^{(1)}r)^2 \,\mathrm{d}r \approx -\pi(c^{(1)})^2 \left[\frac{(\mathrm{d}Q_1/\mathrm{d}r)\,|\psi_1|^2}{|(\mathrm{d}/\mathrm{d}r)(V_1/r)|}\right]_{r=r_c}. \tag{4.10}$$

Equation (4.10) should be treated as an equation for $\mathrm{Im}\, c$. As before, we assume that $V_1(r)$ is a sign-definite function, in which case (4.10) has a solution if and only if $V_1(r)$ and $(\mathrm{d}Q_1/\mathrm{d}r)_{r=r_c}$ are of opposite sign. If they indeed are, two solutions exist for $\mathrm{Im}\, c$, corresponding to two complex-conjugate eigenvalues, one of which is unstable. If, on the other hand, V_1 and $(\mathrm{d}Q_1/\mathrm{d}r)_{r=r_c}$ are of the same sign, no solutions exist for $\mathrm{Im}\, c$. This means that our boundary-value problem does not have eigenvalues (stable or unstable), which should be interpreted as stability.

Observe, however, that the right-hand side of (4.10) depends on the unknown quantities r_c and $(\psi_1)_{r=r_c}$, which do not allow one to find $\mathrm{Im}\, c$. The value of r_c can be determined approximately, by assuming

$$\frac{1}{r_c} V_1(r_c) \approx \varepsilon c^{(1)}. \tag{4.11}$$

The situation with $(\psi_1)_{r=r_c}$ is less straightforward, as its leading-order approximation, $\psi_1^{(0)} = V_1$, is inapplicable near the critical level. It was obtained using the upper-layer equation (3.6), where c was neglected and V_1/r retained, but near the critical level they are of the same order. This inconsistency is difficult to correct, as $(\psi_1)_{r=r_c}$ can be found only using the method of matched asymptotic expansions – not only is this task associated with cumbersome calculations but it also depends on the asymptotics of $V_1(r)$ as $r \to \infty$. The latter makes it impossible to derive a general formula for $(\psi_1)_{r=r_c}$, even though every particular case is (more or less) readily tractable.

In what follows, (4.10)–(4.11) will be used as a stability criterion.

4.4. *Examples*

In order to test a particular vortex profile $V_1(r)$ for stability with respect to mixed modes, one needs to take the following steps:

(i) Solve the first-order boundary-value problem (4.4)–(4.6) and determine the eigenvalues $c^{(1)}$ (in most cases, it is enough to compute the largest eigenvalue, which loses stability first; in other cases, solving (4.4)–(4.6) can be bypassed altogether – see below). However, even though (4.4)–(4.6) always have solutions (modes), the existence of these solutions with respect to higher-order approximations remains to be verified.

(ii) To do so, determine the positions of the critical levels corresponding to the eigenvalues found (i.e. find the points which satisfy condition (4.11)).

(iii) Check the sign of the PV gradient at the critical levels. The modes for which it is opposite to the sign of V_1 indeed exist and have non-zero $\mathrm{Im}\, c$. The modes for which the PV gradient at the critical level and V_1 are of the same sign do not exist as higher-order solutions.

Thus, a vortex is unstable if and only if there exists at least one first-order mode one first-order mode (*solution of* (4.4)–(4.6)), *for which the PV gradient at the critical level is of the opposite sign to that of* V_1.

As the first example, we consider the Gaussian vortex,

$$V_1 = \frac{r}{r_0} \exp\left(-\frac{r^2}{2r_0^2}\right), \tag{4.12}$$

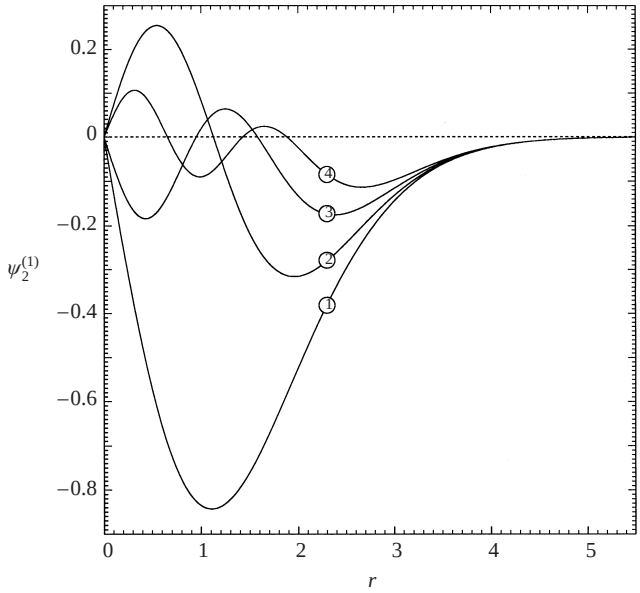

FIGURE 1. The asymptotic lower-layer eigenfunctions (solutions of (4.4)–(4.6)) for the Gaussian vortex (4.12) with $r = 1.5$. The curves are labelled by the mode number.

where r_0 is the radius of maximum swirl velocity. Another important parameter is the depth ratio ε. For the particular case of

$$r_0 = 1.5, \quad \varepsilon = 0.1,$$

several first eigenvalues of the asymptotic boundary-value problem (4.4)–(4.6) were found numerically:

$$c^{(1)} = 0.16795,\ 0.06336,\ 0.03352,\ 0.02079\ \ldots\ .$$

The corresponding eigenfunctions are shown in figure 1 – observe that they satisfy the 'oscillation theorem', i.e. the first eigenfunction (the one corresponding to the largest eigenvalue) has one extremum, the second eigenfunction has two extrema, etc. (this behaviour is typical for second-order equations with regular coefficients). The oscillation theorem allows one to make sure that no eigenvalues have been missed in computation (which is impossible to do for the exact eigenvalue problem). Note also that the oscillation theorem is not applicable to the upper-layer eigenfunction – recall that, to the leading order, $\psi_1^{(0)} = V_1$, which is not oscillatory.

The positions of the critical levels for the above eigenvalues are shown in figure 2(a), and the corresponding values of the PV gradient are shown in figure 2(b). Evidently, all modes are stable. Let us now increase the depth ratio ε, keeping the radius r_0 of the vortex fixed. In this case, the eigenvalues $c^{(1)}$ are also fixed (they depend only on the shape of the vortex), but the 'full' phase speed, $c \approx \varepsilon c^{(1)}$, scales with ε and, hence, grows. As a result, the critical levels move towards the centre of the vortex, where the angular velocity is larger. One after another, they enter the area of negative PV gradient (see figure 2) and, according to our criterion, become unstable. Observe that the first (largest) eigenvalue becomes unstable first, which makes it an 'instability indicator'.

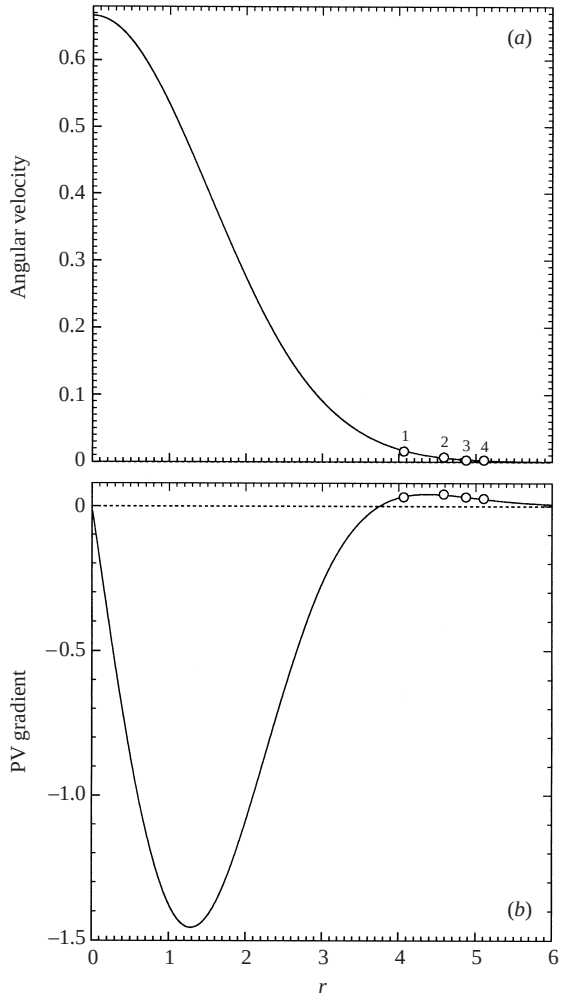

FIGURE 2. The angular velocity (a), and PV gradient (b) of Gaussian vortex (4.12) with $r_0 = 1.5$. Circles show the positions of the critical levels of the first four modes, for the depth ratio $\varepsilon = 0.1$. As the PV gradient at all four critical levels is positive, the corresponding modes are stable.

Next, we shall fix ε and increase r_0. In this case, definition (2.11) of $\mathrm{d}Q_1/\mathrm{d}r$ shows that

$$\frac{\mathrm{d}Q_1}{\mathrm{d}r} \to -V_1 \quad \text{as} \quad r_0 \to \infty. \tag{4.13}$$

Hence, the sign of the PV gradient becomes opposite to that of V_1 (not only at the critical level, but everywhere). We conclude that all large vortices† do *not* satisfy the stability criterion derived (note that (4.13) holds for any vortex shape, not necessarily Gaussian). In other words, a stable vortex could be made unstable by increasing its radius.

The predicted properties of Gaussian vortices have been tested against the exact solution, obtained through numerical integration of equations (3.1)–(3.2), (2.6). As

† Dimensionally, 'large' means $(r_{0*}/L_d)^2 \gg 1$, where r_{0*} is the dimensional radius of the vortex, and L_d is the deformation radius.

we were interested mostly in the cases of marginal stability, where the coefficients of these equations are singular (at the critical levels), we used a numerical method based on extending the spatial variable r to the complex plane (see Appendix C).

First, we checked that the first mixed mode indeed becomes unstable before all other mixed modes, and the exact solution did confirm this asymptotic conclusion. On increasing r_0 or ε, the second and further modes soon follow, but their growth rates still remain smaller than that of the first mode.

Secondly, we computed the marginal stability curve, separating the regions of stability and instability with respect to the first mixed mode, on the (ε, r_0)-plane (figure 3*a*). One can see that the asymptotic and exact curves agree reasonably well for $\varepsilon \lesssim 0.2$ (as they should). It is also worth noting that no modes, other than mixed modes, were found for $k = 1$. (It will be proven in § 5 that LLD modes do not exist for $k = 1$; and neither do ULD modes, as mentioned by Paldor (1999)†.)

We have also examined the profile

$$V_1 = \frac{r}{r_0}\operatorname{sech}\left(\frac{r}{r_0}\right), \tag{4.14}$$

which will be referred to as the 'Sech profile'. The most important feature of this vortex is that

$$\text{if } r_0 > 1, \quad \frac{\mathrm{d}Q_1}{\mathrm{d}r} < 0 \quad \text{for all } r.$$

Hence, vortices with $r_0 \geqslant 1$ are unstable for any ε (in this case, no matter where the critical levels are, the PV gradient there is negative). Furthermore, even after r_0 has crossed the threshold value of $r_0 = 1$, the instability cannot disappear immediately – as a result, the stability region on the (ε, r_0)-plane for the Sech vortex is relatively small (compare figures 3*a* and 3*b*). Interestingly, the asymptotic and exact marginal stability curves for the Sech vortex coincide remarkable well, and not only for small ε, but also for $\varepsilon \sim 1$ (see figure 3*b*). Otherwise, the Sech vortex is similar to the Gaussian vortex, including the property of the first mixed mode becoming unstable before the other mixed modes.

It is worth noting that there are important classes of vortex profiles which can be tested for stability without actually solving the first-order boundary-value problem. Indeed, consider, for example, a vortex with algebraic periphery,

$$V_1 \to \left(\frac{r}{r_0}\right)^{-n} \quad \text{as} \quad r \to \infty. \tag{4.15}$$

Calculating the asymptotics of the PV gradient,

$$\frac{\mathrm{d}Q_1}{\mathrm{d}r} \to (n^2 - 1)\left(\frac{r}{r_0}\right)^{-n-2} - \left(\frac{r}{r_0}\right)^{-n} \approx -\left(\frac{r}{r_0}\right)^{-n} \quad \text{as} \quad r \to \infty,$$

one can see that its sign is opposite to that of V_1. Hence, any mode with sufficiently large coordinate of its critical level is unstable. And, of course, there are plenty of such modes, as the asymptotic boundary-value problem has an infinite sequence of solutions with phase speeds tending to zero (accordingly, the coordinates of the critical levels tend to infinity). It should be noted though that the growth rate of these higher modes is small, as their critical levels are located very far from the vortex core, where the eigenfunction is small.

† Strictly speaking, Paldor's (1999) claim was made for the equation describing barotropic disturbances on a barotropic vortex, but mathematically it coincides with our equation (3.3).

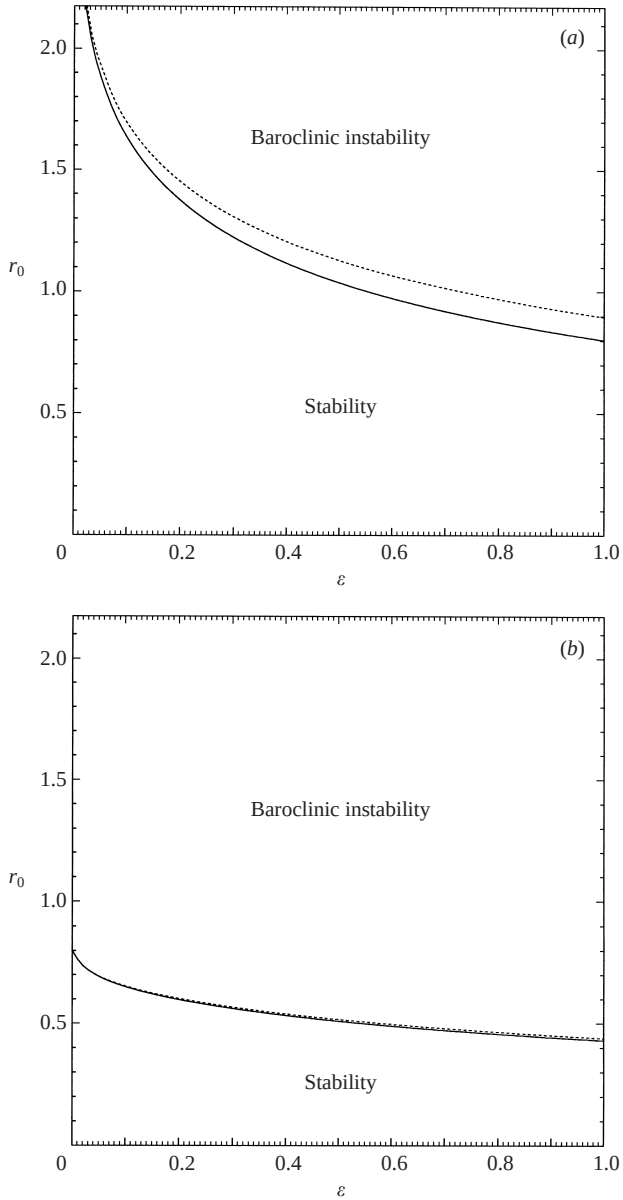

FIGURE 3. The curves of marginal stability with respect to the mixed mode $k = 1$. The solid line shows the exact solution, the dotted line shows the asymptotic solution (obtained for the limit $\varepsilon \to 0$). (*a*) Gaussian vortices (4.12); (*b*) Sech vortices (4.14).

Summarizing the results of this subsection, we note that a connection can be drawn between the large-distance asymptotics of the vortex and its stability properties. Indeed, the strongly decaying Gaussian vortex is the most stable of the three examples considered, whereas the slowly decaying algebraic vortex is the most unstable one. Overall, the crucial importance of the vortex periphery is not all that surprising, as that is where the critical levels are located.

Having concluded that instability of thin vortices is caused by critical levels, we shall now discuss the contradiction between the results of Ripa (1992) and Paldor

& Nof (1990), regarding vortices with constant angular velocity. The crucial point here is that they do not have critical levels, hence should be stable (provided they are thin, of course, otherwise our results are not applicable). This appears to resolve the contradiction in favour of Paldor & Nof (1990), although a conclusive answer can be obtained only after we extend our approach to ageostrophic vortices (for which both conflicting results have been obtained). Indeed, it is possible, in principle, that ageostrophic effects give rise to an essentially ageostrophic unstable mode, which is beyond the scope of our QG analysis.

Finally, we note that instability of vortices with respect to the first azimuthal wavenumber $k = 1$ is sometimes believed not to inflict structural damage to the vortex, but rather make it move laterally as a solid. This does not seem to be relevant on the present case. First, only the leading-order eigenfunction corresponds to a shift of the vortex as a whole, whereas the higher approximations do not. Secondly, the frequency in the present case has a sizeable real part, which corresponds to periodic oscillations of the vortex about a certain point. Since the frequency has an imaginary part as well, the amplitude of the oscillations grows, and so does the dipole component of the flow associated with the oscillations (the dipole component is, essentially, what makes the vortex move). Eventually, it is difficult to imagine that the growing dipole component can leave the vortex intact.

It should be admitted though that a conclusive answer to the question of long-term evolution of a ($k = 1$)-unstable vortex can be given only by simulations of the original nonlinear equations. For the present work, however, this issue is not overly important, as the vortices under consideration are also unstable with respect to $k \geqslant 2$ (see § 5).

4.5. *Discussion: Why do critical levels destabilize the vortex?*

In this subsection, we shall briefly discuss why critical levels are so important for stability properties of vortices.

The answer to this question can be found in the paper by Timofeev (1970), where it was demonstrated that an extensive exchange of momentum between the mean flow and disturbances occurs at critical levels. As a result, a disturbance may gain momentum and grow. It should be emphasized, however, that the mere existence of a critical level is not enough to cause instability, as the momentum given by the mean flow is not necessarily of the same sign as that of the disturbance, i.e. instead of causing growth it may cause decay.

It would be interesting to interpret our instability criterion in terms of angular momentum exchange at critical levels (this work is in progress).

5. Lower-layer-dominated modes

LLD modes are described by the asymptotic equations (3.4)–(3.5), which are to be solved with the usual boundary conditions,

$$\psi_1^{(0)}(0) = \psi_1^{(0)}(\infty) = 0, \quad \psi_2^{(0)}(0) = \psi_2^{(0)}(\infty) = 0. \tag{5.1}$$

5.1. *Analytical results*

It turns out that, in a sense, LLD and mixed modes complement each other: the latter exist only for the first azimuthal wavenumber $k = 1$, whereas the former exist only for the higher wavenumbers $k \geqslant 2$:

The LLD boundary-value problem (3.4)–(3.5), (5.1) *has no solution for* $k = 1$.

In order to prove this statement, observe that

$$\psi_2^{(0)} \to \text{const}_1\, r^k + \frac{\text{const}_2}{r^k} \quad \text{as} \quad r \to \infty,$$

which follows from the lower-layer equation (3.5). The boundary conditions imply that $\text{const}_1 = 0$; we can also put (without loss of generality) $\text{const}_2 = 1$ and obtain

$$\psi_2^{(0)} \to \frac{1}{r^k} \quad \text{as} \quad r \to \infty. \tag{5.2}$$

Now, multiply (3.4) by r and integrate over $0 < r < \infty$. After integration by parts and straightforward algebra, we obtain

$$\int_0^\infty r V_1 \psi_2^{(0)}\, \mathrm{d}r = \int_0^\infty \frac{k^2 - 1}{r} V_1 \psi_1^{(0)}\, \mathrm{d}r.$$

Next, we multiply (3.5) by r^{k+1} and integrate over $0 < r < \infty$. Integrating by parts and using condition (5.2), we obtain

$$\int_0^\infty r^k V_1 \psi_2^{(0)}\, \mathrm{d}r = 2c^{(1)}.$$

Comparing the last two identities for $k = 1$, one can see that they are inconsistent, unless $c^{(1)} = 0$ – which, in turn, entails $\psi_2^{(0)} = 0$ (see (3.5)), and, hence, cannot hold for an LLD mode (it should be recalled that, by definition, LLD modes have non-zero leading-order amplitude in the lower layer).

Similarly to the mixed-mode case, it can be further proven that the asymptotic boundary-value problem for LLD modes has only real eigenvalues, which are of the same sign as that of V_1. Hence, their stability properties depend on the structure of the critical layer. In order to clarify that, we shall again simplify identity (2.2) by putting

$$\psi_2 \approx \psi_2^{(0)}, \quad \text{Re}\, c \approx \varepsilon c^{(1)}. \tag{5.3}$$

It should be observed, however, that, in the present case, the lower-layer eigenfunction is greater than that for mixed modes (compare (5.3) to (4.7)). As a result, the LLD equivalent of (4.10) is

$$|\text{Im}\, c| \int_0^\infty V_1 (\psi_2^{(0)})^2\, \mathrm{d}r \approx -\pi (\varepsilon c^{(1)})^2 \left[\frac{\mathrm{d}Q_1/\mathrm{d}r\, |\psi_1|^2}{|(\mathrm{d}/\mathrm{d}r)(V_1/r)|} \right]_{r=r_c}. \tag{5.4}$$

Equation (5.4) should be treated as an equation for $\text{Im}\, c$: existence of solutions proves instability, absence of solutions proves stability. Hence, the stability criterion for LLD modes is exactly the same as that for mixed modes: the vortex is stable if and only if the sign of $(\mathrm{d}Q_1/\mathrm{d}r)_{r=r_c}$ coincides with that of V_1.

5.2. *Examples and discussion*

The above criterion has been tested against the exact marginal stability curve computed numerically for $k = 2$, for the Gaussian and Sech vortices. As before, the mode with the largest value of $\text{Re}\, c$ always becomes unstable before the other modes with the same value of k, and fast-decaying profiles are more stable than slowly decaying profiles (which, of course, should have been expected, as the stability criterions for LLD and mixed modes are essentially the same).

Interestingly, in the Gaussian case, the LLD instability cannot be completely separated from the ULD instability. There is no problem, of course, with separating the two types of instability for small ε; if, however, the layers are of comparable depths, the disturbance cannot be localized in a single layer. Therefore, it comes as no surprise that the two (exact) marginal stability curves meet at $\varepsilon \approx 0.88$ (see figure 4*a*). Having this in mind, we have computed the asymptotic curve of marginal stability for ULD modes as well (based on the equivalent-barotropic equation (3.3)). It can be seen that, although the asymptotic curves of ULD and LLD modes do not meet at $\varepsilon \sim 1$, they work reasonably well for $\varepsilon \lesssim 0.2$.

It is interesting to interpret the results presented in figure 4(*a*) in terms of barotropic and baroclinic instabilities. Consider, for example, a stable vortex within the stability region in figure 4(*a*). If we begin to decrease its radius, sooner or later we reach the area of instability caused by strong *horizontal* shear – hence, it should be interpreted as equivalent-barotropic instability. If we go in the opposite direction, i.e. increase the radius of the vortex, it also becomes unstable. In this case, the horizontal shear is weak, and the instability is caused by *vertical* shear – hence, it should be interpreted as baroclinic instability. Observe that, even though *strong* horizontal shear causes instability, *moderate* horizontal shear inhibits it (that is what stabilizes vortices with moderate values of r_0). This probably occurs because horizontal shear tilts the interface, emulating the stabilizing effects of a sloping bottom or the beta-effect.

We have also computed the $k = 2$ stability curve for the Sech vortex (see figure 4*b*). Unlike its Gaussian counterpart, the Sech vortex turned out to be barotropically stable no matter how small r_0 is. In general, it appears that slowly decaying vortices are more stable *barotropically* than fast-decaying vortices (which is the opposite to how the structure of the vortex's periphery affects *baroclinic* instability). This conclusion agrees with the results obtained for a particular case of an (slowly decaying) algebraic vortex,

$$V_1 = \frac{r}{r_0}\left[1 + \left(\frac{r}{r_0}\right)^2\right]^{-3},$$

which turned out to be barotropically stable, but unstable baroclinically for all r_0 and ε. On the other hand, a particular case of a vortex with finite support,

$$V_1 = \begin{cases} \dfrac{r}{r_0}\left[1 - \left(\dfrac{r}{r_0}\right)^2\right]^3 & \text{if} \quad r < r_0, \\ 0 & \text{if} \quad r \geqslant r_0, \end{cases}$$

turned out to be relatively stable baroclinically, but very unstable barotropically (as a result the two areas of instability close up and leave no stability region on the (ε, r_0)-plane at all). We conclude that the models of algebraic and finite-support vortices are not relevant to the real ocean.

Finally, we shall discuss which of the three types of instability (ULD, LLD, or mixed) is the strongest one and, hence, the most important. At a first glance, the obvious candidate for the strongest instability is the equivalent-barotropic (ULD) instability. Indeed, the growth rate of ULD modes scales with unity, whereas the growth rates of the two slow types are much weaker (that is, weaker for thin vortices, of course). However, ULD disturbances become unstable only for relatively small r_0: for example, for the Gaussian profile the threshold value is $r_0 \sim 0.5$, which, dimensionally, corresponds to just half of the deformation radius. Indeed, none of the 35 oceanic rings catalogued by Olson (1991) come even close to being barotropically

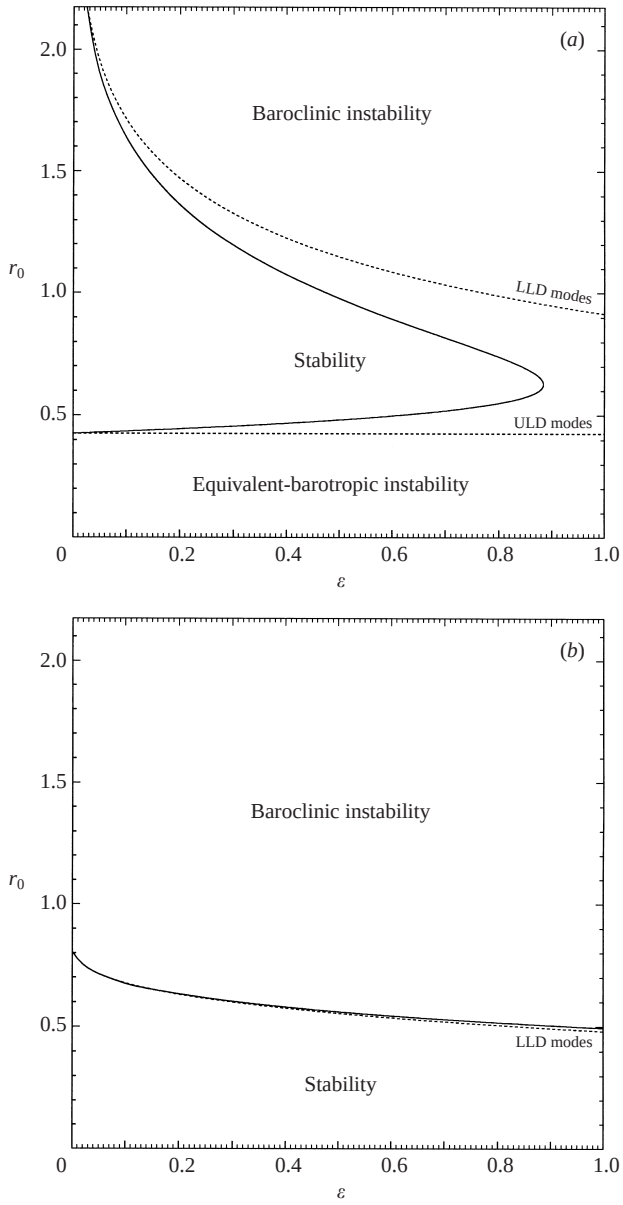

FIGURE 4. The curves of marginal stability with respect to upper/lower-layer-dominated modes with $k = 2$. The solid line shows the exact solution, the dotted line shows the asymptotic solution (obtained for $\varepsilon \ll 1$). (*a*) Gaussian vortices (4.12); (*b*) Sech vortices (4.14).

unstable within the framework of the Gaussian model (among the 35 rings, the smallest value of r_0 is 0.81).†

The remaining (LLD and mixed) types of instability will be compared in two ways. First, we compare their marginal stability curves. Surprisingly, the curves for mixed modes ($k = 1$) and for LLD modes with $k = 2$ turned out to be remarkably close for

† It should be noted, however, that Olson's (1991) paper was focused on the so-called rings, which are the largest of oceanic eddies. However, smaller vortices have also been observed in the ocean (e.g. D'Asaro 1988), and those, of course, can be unstable barotropically.

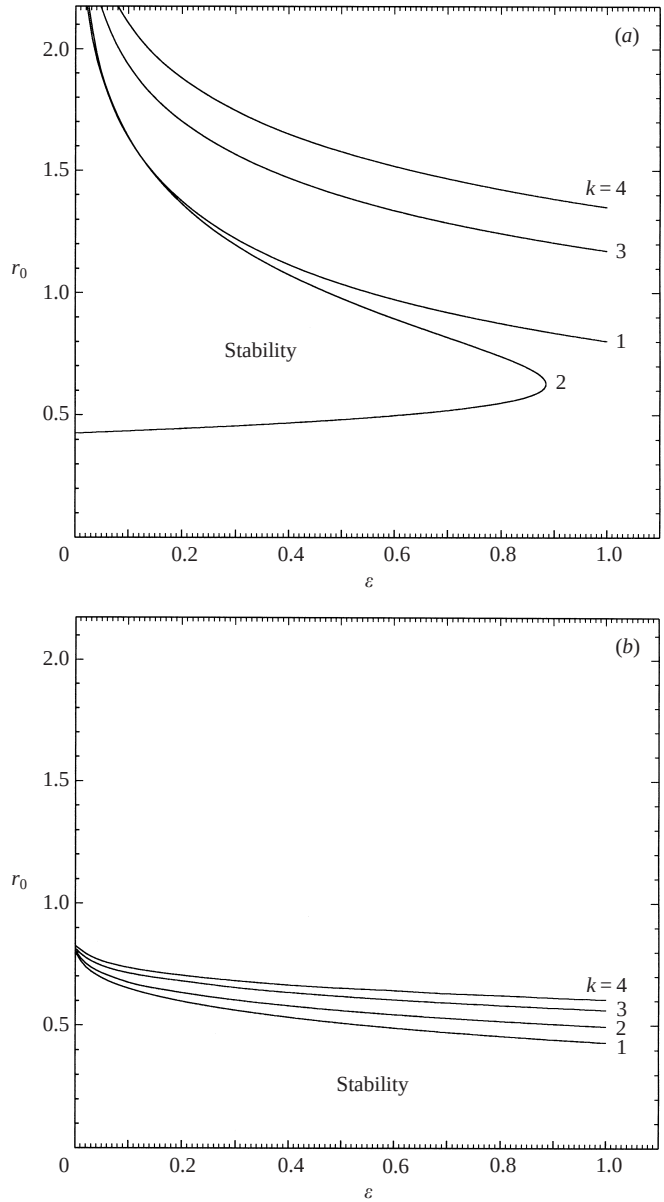

FIGURE 5. The (exact) curves of marginal stability with respect to modes with $k = 1, 2, 3, 4$. (*a*) Gaussian vortices (4.12); (*b*) Sech vortices (4.14).

$\varepsilon \lesssim 0.5$ for both Gaussian and Sech vortices (see figure 5). The higher-k ($k \geqslant 3$) LLD modes do not affect the region of global stability, as their curves of marginal stability are located entirely within the instability region of the two low-k modes.

Secondly, we have compared the growth rates of mixed and LLD modes. Consider, for example, a marginally stable Sech vortex and begin to increase its radius (see figure 6*b*). In this case, the mixed mode ($k = 1$) becomes unstable first and dominates the instability for some time. The LLD mode with $k = 2$ becomes unstable a little later, but soon overtakes the mixed mode – only to be itself overtaken by the LLD mode with $k = 3$. This pattern can be extended further, with the obvious conclusion

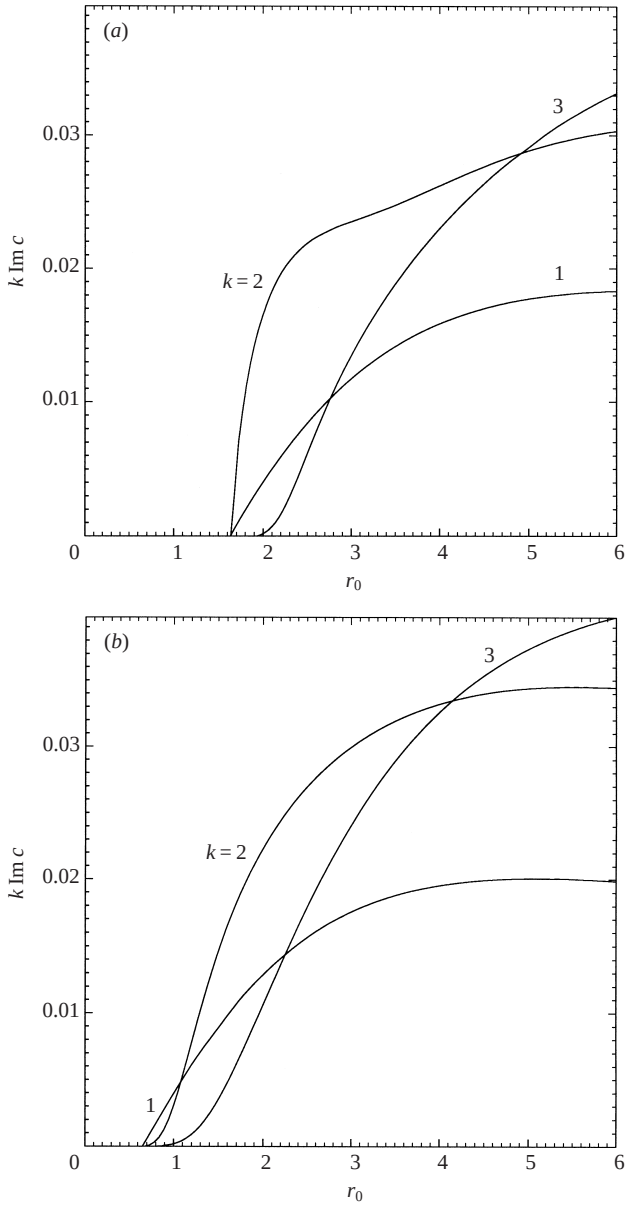

FIGURE 6. The (exact) growth rates of the modes with $k = 1, 2, 3$. The depth ratio is $\varepsilon = 0.1$. (*a*) Gaussian vortices (4.12); (*b*) Sech vortices (4.14).

that large vortices are mostly unstable with respect to higher-k modes. This is also true for Gaussian vortices, with the only exception that the two low-k modes in this case become unstable almost simultaneously, and the mixed mode is never the most unstable one (see figure 6*a*).

6. Comparison with observations

As mentioned above, the Gaussian vortex is the most stable out of all profiles considered. Still, it comes a little short of describing the stability properties of real oceanic vortices.

In order to compare our conclusions with observations, we used the results by Olson (1991), who catalogued 35 oceanic rings. Unfortunately, the depth ratio ε, which is one of the two important parameters (the other one is r_0), is not provided in that paper. We can only assume that

$$0.05 \lesssim \varepsilon \lesssim 0.1. \tag{6.1}$$

On the basis of this estimate and the marginal stability curves for the Gaussian vortex (figure 5*a*), we conclude that only six rings out of 35 are unconditionally stable, i.e. their radii are small enough to make them baroclinically stable for any ε within the above range. Another three vortices are stable at least for some values of ε within the above range, while the remaining 26 are unconditionally unstable.

We have also computed (using the exact equations) the growth rate of the instability for a vortex of 65 km in radius (which is the average radius of the rings described by Olson 1991), in the ocean with deformation radius of 27 km (which is, again, an average derived from Olson's data). As mentioned above, Olson provides no information about the depth ratio, and we chose the most unstable value of range (6.1), $\varepsilon = 0.1$. Olson does provide the maximum velocity of the vortex, but we need the maximum value of the velocity averaged over the depth of the upper layer (which is the price we have to pay for using the two-layer model). Estimating it to be within the range of 0.1–0.25 m s^{-1}, we obtain the e-folding time of the instability within the range of 89–36 days. This, probably, can explain why a vortex may look steady while it is being measured (and then reported in the literature as existing in the ocean); but it, clearly, contradicts the fact that some of the oceanic vortices last for up to 3 years.

There are three possible explanations of this result. First, a vortex profile may exist which is more stable than the Gaussian profile for larger vortices. Secondly, it is unclear how Olson (1991) defined the upper-layer deformation radius L_d for the continuously stratified real ocean. As a result, the non-dimensional radius of the ring derived from Olson's data may be larger than what it was in reality (and larger vortices are, generally, more unstable). Thirdly, our model assumes that the vortex does not penetrate into the lower layer, and it is unclear how a deep circulation would affect the stability of the vortex. Particular cases examined numerically by Dewar & Killworth (1995) suggest that even a weak co-rotating circulation in the lower layer can stabilize a vortex.

7. Summary and concluding remarks

Thus, we have examined the stability of quasi-geostrophic vortices localized in a thin upper layer of a two-layer ocean. We assumed the disturbance to be harmonic and reduced the governing equations to a boundary-value problem (3.1)–(3.2), (2.6). The usual (based on monotonicity of PV) criterion of stability turned out to be useless (§ 2.2), and the solution to the boundary-value problem was sought asymptotically, as an expansion in powers of the depth ratio $\varepsilon = H_1/H_2$.

The results obtained can be subdivided into four categories.

(*a*) A complete classification of the modes of the problem has been developed (§ 3, see also table 1). The properties of slow (mixed and LLD) modes, responsible for baroclinic instability, have been examined in §§ 4–5, whereas fast (ULD) modes, responsible for equivalent-barotropic instability, appear to be unimportant oceanographically (they exist only for unrealistically small vortices, with a radius smaller than half of the deformation radius).

	ψ_1	ψ_2	$\mathrm{Re}\, c$	$k\mathrm{Im}\, c$	k
Upper-layer-dominated modes	$O(1)$	$O(\varepsilon)$	$O(1)$	$O(1)$	$k \geqslant 2$
Lower-layer-dominated modes	$O(1)$	$O(1)$	$O(\varepsilon)$	$o(\varepsilon)$	$k \geqslant 2$
Mixed modes	$O(1)$	$O(\varepsilon)$	$O(\varepsilon)$	$o(\varepsilon)$	$k = 1$

TABLE 1. The properties of the normal modes. $\psi_{1,2}$ are the amplitudes of the streamfunctions in the upper and lower layers, ε is the depth ratio, $\mathrm{Re}\, c$ is the angular phase velocity, $k\,\mathrm{Im}\, c$ is the growth rate, and k is the azimuthal wavenumber.

The classification of modes is the foundation of all results obtained in this paper. Not only has it been used in our asymptotic analysis, but it also helped to interpret the results of numerical solution of the exact equations.

(*b*) We have derived an asymptotic criterion of stability for mixed and LLD modes. In order to test a particular vortex profile $V_1(r)$ for stability, one needs to take the following steps:

(i) Determine the first-order eigenvalues $c^{(1)}$ (for mixed modes, they are described by equations (4.4)–(4.6), and for LLD modes by (3.4)–(3.5), (5.1)). It should be kept in mind that, even though the first-order equations always have an infinite number of solutions (modes), the existence of these solutions with respect to higher-order approximations remains to be verified.

(ii) To do so, determine the positions of the critical levels corresponding to the eigenvalues found, i.e. find the points r_c which satisfy

$$\frac{1}{r_c} V_1(r_c) = \varepsilon c^{(1)}$$

(V_1/r is assumed monotonic, hence there is only one critical level per mode). Most importantly, the presence of ε on the right-hand side of this equation indicates that critical levels are located at the periphery of the vortex, where the angular velocity is small (this applies, of course, only to thin vortices and slow modes).

(iii) Determine the sign of the upper-layer PV gradient,

$$\frac{\mathrm{d}Q_1}{\mathrm{d}r} = \frac{\mathrm{d}}{\mathrm{d}r}\left[\frac{1}{r}\frac{\mathrm{d}}{\mathrm{d}r}(rV_1)\right] - V_1,$$

at the modes critical levels. The modes, for which it is opposite to the sign of V_1, do exist and have non-zero $\mathrm{Im}\, c$. The modes, for which $(\mathrm{d}Q_1/\mathrm{d}r)_{r=r_c}$ and V_1 are of the same sign, do not exist as higher-order solutions.

Thus, a vortex is unstable if and only if there exists one or more first-order solutions, for which the sign of the PV gradient at the critical level is opposite to that of V_1.

It is worth elaborating why the first-order boundary-value problem is simpler than the exact equations. To begin with, the former has regular coefficients (singularities associated with critical levels appear in higher orders). In addition, its solutions satisfy the 'oscillation theorem', i.e. the first eigenfunction (the one corresponding to the largest eigenvalue) has one extremum, the second eigenfunction has two extrema, etc., which allows one to make sure that no eigenvalues have been missed in computation. (With the exact equations, one can never be sure that all modes have been computed, which makes it difficult to prove stability.) Note also that, in most cases, it is enough to compute the largest $c^{(1)}$ only, as it usually loses stability first; in other cases, solving the first-order equations can be bypassed altogether.

(*c*) This brings us to the third group of results: using the asymptotic stability criterion, we have examined the stability properties of several classes of vortex profiles in a wide range of parameters. In general, there is a link between the stability properties of the vortex and the structure of its periphery (simply because the latter is where the critical levels are located). Vortices with a slowly decaying periphery are more baroclinically unstable than vortices with a fast-decaying periphery. As a result, the Gaussian vortex,

$$V_1 = \frac{r}{r_0} \exp\left(-\frac{r^2}{2r_0^2}\right),$$

is more stable than the 'Sech vortex',

$$V_1 = \frac{r}{r_0} \operatorname{sech}\left(\frac{r}{r_0}\right)$$

(see the marginal stability curves in figure 5); and the Sech vortex, is more stable than vortices with algebraic periphery,

$$V_1 \to \left(\frac{r}{r_0}\right)^{-n} \quad \text{as} \quad r \to \infty$$

(which are always unstable).

Interestingly, this conclusion applies only to baroclinic instability (i.e. instability with respect to LLD and mixed modes). In the case of equivalent-barotropic (ULD) instability, the tendency is opposite: vortices with a slowly decaying periphery are more stable than those with a fast-decaying periphery. Accordingly, the Sech vortex is barotropically stable no matter how small its radius is, and the Gaussian vortex is unstable only for some (small) values of r_0, whereas the following example of a 'vortex with finite support':

$$V_1 = \begin{cases} \dfrac{r}{r_0}\left[1 - \left(\dfrac{r}{r_0}\right)^2\right]^3 & \text{if} \quad r < r_0, \\ 0 & \text{if} \quad r \geqslant r_0, \end{cases}$$

is barotropically unstable over a wide range of parameters. Overall, baroclinically and barotropically, the Gaussian vortex is the most stable one out of all profiles considered.

(*d*) Finally, the fourth group of results obtained in this paper is associated with the numerical method used for solving the exact boundary-value problem. The main difficulty in solving this and other problems of hydrodynamic stability is associated with critical levels. In order to calculate the marginal stability curve (which is the most important characteristic of instability), one has to deal with the cases where $\operatorname{Im} c = 0$ and the equations have singularities at critical levels. This is a well-known problem, it has been mentioned, in particular, by Ikeda (1981), who had to 'manually' extrapolate $\operatorname{Im} c$ from the cases where it is non-zero.

In the present paper, the singularity associated with the case of neutral stability was treated using the extension of the spatial variable r to complex values. In this case, one is not restricted to the physical path of integration (along the real axis), but can choose any path, provided it can be continuously transformed into the physical one without crossing the singular points of the equations' coefficients. As a result, one can choose a path which lies far away from all singularities. For further details, we refer the reader to Appendix C, and only mention that numerical integration of the exact equations confirms that the asymptotic stability criterion works well for $\varepsilon \lesssim 0.2$, which covers all oceanographically interesting cases.

Appendix A. Reduction of (4.4)–(4.6) to a 'usual' boundary-value problem

There are two features that make boundary-value problem (4.4)–(4.6) unusual: the non-homogeneous term V_1 in (4.4) and the integral nature of condition (4.5). Both can be changed to a more traditional form in the general case. However, we shall confine ourselves to the (particularly simple) case where $V_1(r)$ is a function with compact support, i.e.

$$V_1 = 0 \quad \text{for} \quad r > R.$$

Observe that, in the context of numerical solution, this case is as good as general, as one has to truncate the numerical solution somewhere anyway. Then, for $r > R$, equation (4.4) becomes

$$\frac{1}{r}\frac{\mathrm{d}}{\mathrm{d}r}\left(r\frac{\mathrm{d}\psi_2^{(1)}}{\mathrm{d}r}\right) - \frac{1}{r^2}\psi_2^{(1)} = 0,$$

and can be readily solved:

$$\psi_2^{(1)} = \frac{\text{const}}{r} \quad \text{for} \quad r > R.$$

Using this solution, the boundary condition at $r = \infty$ can be moved to $r = R$. To do so, observe that $\psi_2^{(1)}$ and its derivative should be continuous:

$$\psi_2^{(1)} = \frac{\text{const}}{R}, \quad \frac{\mathrm{d}\psi_2^{(1)}}{\mathrm{d}r} = -\frac{\text{const}}{R^2} \quad \text{at} \quad r = R.$$

Eliminating the constant, we obtain

$$\psi_2^{(1)} + R\frac{\mathrm{d}\psi_2^{(1)}}{\mathrm{d}r} = 0 \quad \text{at} \quad r = R. \tag{A 1}$$

Next, we replace $\psi_2^{(1)}$ with

$$\phi = \psi_2^{(1)} + c^{(1)}r. \tag{A 2}$$

Substituting (A 2) and (4.4)–(4.6) we obtain

$$c^{(1)}\left[\frac{1}{r}\frac{\mathrm{d}}{\mathrm{d}r}\left(r\frac{\mathrm{d}\phi}{\mathrm{d}r}\right) - \frac{1}{r^2}\phi\right] + \frac{1}{r}\phi V_1 = 0, \tag{A 3}$$

$$\phi = 0 \quad \text{at} \quad r = 0, \tag{A 4}$$

$$\phi + R\frac{\mathrm{d}\phi}{\mathrm{d}r} = 2c^{(1)}R \quad \text{at} \quad r = R, \tag{A 5}$$

$$\int_0^\infty rV_1\phi\,\mathrm{d}r = 0. \tag{A 6}$$

Now, consider the following combination of (A 3) and (A 6):

$$\int_0^\infty (\text{A 3})\,r^2\,\mathrm{d}r - (\text{A 6}).$$

Integrating by parts, we obtain

$$R\frac{\mathrm{d}\phi}{\mathrm{d}r} - \phi = 0 \quad \text{at} \quad r = R. \tag{A 7}$$

This boundary condition can replace the integral condition (A 6).

Finally, observe, that the 'normalizing' condition (A 5) does not affect the eigenvalue $c^{(1)}$ and, in principle, can be omitted. The boundary-value problem will then consist of (A 3), (A 4), and (A 7).

Appendix B. Properties of the eigenvalues of (4.4)–(4.6)

Rewrite (4.4)–(4.5) in the form

$$c^{(1)}\left[\frac{1}{r}\frac{\mathrm{d}}{\mathrm{d}r}\left(r\frac{\mathrm{d}\phi}{\mathrm{d}r}\right)-\frac{1}{r^2}\phi\right]+\frac{1}{r}V_1\phi=0, \tag{B 1}$$

$$\int_0^\infty rV_1\phi\,\mathrm{d}r=0, \tag{B 2}$$

where

$$\phi=\psi_2^{(1)}+c^{(1)}r. \tag{B 3}$$

Then, it follows from (B 1) that

$$\phi\to A\,r+B\,r^{-1}+o(r^{-2}), \tag{B 4}$$

where A and B are constants. It can be further deduced from (B 3) that

$$A=c^{(1)}. \tag{B 5}$$

In order to determine B, multiply (B 1) by r^2 and integrate from $r=0$ to $r=R$:

$$c^{(1)}\left(r^2\frac{\mathrm{d}\phi}{\mathrm{d}r}-r\phi\right)_{r=R}+\int_0^R rV_1\phi\,\mathrm{d}r=0.$$

Taking the limit $R\to\infty$ and taking into account (B 2), (B 4), we obtain

$$B=0. \tag{B 6}$$

Now, it follows from (B 4)–(B 6) that

$$r\frac{\mathrm{d}\phi}{\mathrm{d}r}\to\phi+o(r^{-2})\quad\text{as}\quad r\to\infty \tag{B 7}$$

(this condition will be used later).

Next, multiply (B 1) by $r\phi^*$ and integrate from $r=0$ to $r=R$:

$$c^{(1)}\left[\left(r\phi^*\frac{\mathrm{d}\phi}{\mathrm{d}r}\right)_{r=R}-\int_0^R\left(r\left|\frac{\mathrm{d}\phi}{\mathrm{d}r}\right|^2+\frac{1}{r}|\phi|^2\right)\mathrm{d}r\right]+\int_0^R V_1|\phi|^2\,\mathrm{d}r=0.$$

Considering the limit $R\to\infty$ and taking into account (B 7), we obtain

$$c^{(1)}\left[\left(|\phi|^2\right)_{r=R}-\int_0^R\left(r\left|\frac{\mathrm{d}\phi}{\mathrm{d}r}\right|^2+\frac{1}{r}|\phi|^2\right)\mathrm{d}r\right]+\int_0^R V_1|\phi|^2\,\mathrm{d}r\to 0\quad\text{as}\quad R\to\infty.$$

Then, using the obvious identity

$$(|\phi|^2)_{r=R}=\int_0^R\left(\frac{\mathrm{d}\phi}{\mathrm{d}r}\phi^*+\frac{\mathrm{d}\phi^*}{\mathrm{d}r}\phi\right)\mathrm{d}r,$$

and taking the limit $R\to\infty$, we obtain

$$c^{(1)}\int_0^\infty r\left|\frac{\mathrm{d}\phi}{\mathrm{d}r}-\frac{1}{r}\phi\right|^2\mathrm{d}r=\int_0^\infty V_1|\phi|^2\,\mathrm{d}r. \tag{B 8}$$

Thus,

$$c^{(1)}=\frac{\text{real quantity}}{\text{another real quantity}},$$

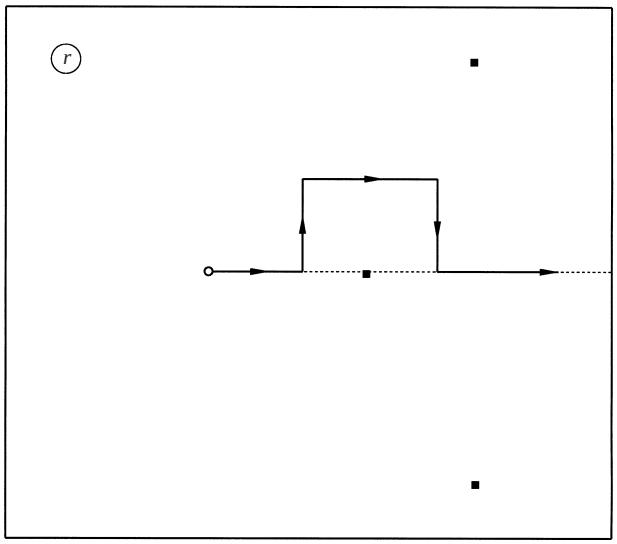

FIGURE 7. The path of integration on the complex r-plane, for the case where one of the critical levels (shown by black squares) approaches the real axis (shown by the dotted line).

which proves that $c^{(1)}$ is real. To complete the proof, we need to demonstrate that the 'other real quantity' may not be zero, i.e.

$$\int_0^R r \left| \frac{\mathrm{d}\phi}{\mathrm{d}r} - \frac{1}{r}\phi \right|^2 \mathrm{d}r \neq 0.$$

Indeed, this would hold unless

$$\phi = A\, r \quad \text{for all } r,$$

which, in turn, holds only in the trivial case of

$$V_1 = 0, \quad \psi_2^{(1)} = 0 \quad \text{for all } r$$

(see (B 1)).

Appendix C. Numerical method for neutrally stable modes

For complex c, the exact equations (3.1)–(3.2) have two singular points: $r = 0$ and $r = \infty$. As the boundary conditions are set precisely at those points, we could not 'shoot' the solution from one of them and adjust c by trying to satisfy the condition at the other. Instead, the solution should be shot from the two boundaries simultaneously and matched at one of the internal points. (In order to shoot the solution from $r = \infty$, one needs to calculate its large-distance asymptotics and use it to set a boundary condition at a large, but finite r.)

If, however, c is real, the equations become singular at yet another point, namely at the critical level: if $\mathrm{Im}\, c = 0$, the denominator of the second term of (2.7) vanishes when

$$\frac{1}{r} V_1(r) = c. \tag{C 1}$$

Theoretically, the singularity should be treated as if c had an infinitesimal imaginary part, using which one could calculate the structure of the eigenfunction near the

critical level and match it to the numerical solution in the outer region (this algorithm was used for a similar, but simpler problem by Benilov (1995)). Unfortunately, the numerical solution cannot approach the critical level too closely and, to maintain accuracy, one needs to calculate many terms in the expansion of the eigenfunction about r_c, which is time-consuming and tedious.

Instead, one can extend the equations and their solution to the plane of complex r and modify the path of integration in such a way that it bypasses the critical level (this approach was initially used by Boyd 1985 for a Chebyshev numerical method, and by Benilov & Sakov 1999 for the Runge–Kutta method, as in this paper). One would still have to keep the endpoints fixed, and also make sure that the modified path can be transformed back to the real axis without touching any of the singular points of the equation. This would guarantee that the solution would arrive at its final destination with the correct value.

In order to illustrate this algorithm, consider the Gaussian profile with $r_0 = 1$,

$$V_1 = r \exp\left(-\frac{r^2}{2}\right), \tag{C 2}$$

and $c = 0.5 + 0.01\,\mathrm{i}$. Equation (C 1) with the left-hand side determined by (C 2) has an infinite number of solutions

$$r = \pm\sqrt{-2\ln c + 2\mathrm{i}\pi n}, \quad n = 0, \pm 1, \pm 2 \ldots,$$

one of which (the closest to $\sqrt{-2\ln|c|}$) represents the physical critical level.

An example of a modified path of integration for this case can be seen in figure 7.

REFERENCES

Andrews, D. G. & McIntyre, M. E. 1976 Planetary waves in horizontal and vertical shear: the generalized Eliassen–Palm relation and the mean zonal acceleration. *J. Atmos. Sci.* **33**, 2031–2048.

Benilov, E. S. 1995 On the instability of large-amplitude geostrophic flows in a two-layer fluid: the case of 'strong' beta-effect. *J. Fluid Mech.* **284**, 137–158.

Benilov, E. S., Broutman, D. & Kuznetsova, E. P. 1998 On the stability of large-amplitude vortices in a continuously stratified fluid on the f-plane. *J. Fluid Mech.* **355**, 139–162.

Benilov, E. S. & Sakov, P. V. 1999 On the linear approximation of velocity and density profiles in the problem of baroclinic instability. *J. Phys. Oceanogr.* **29**, 1374–1381.

Boyd, J. 1985 Complex coordinate methods for hydrodynamics instabilities and Sturm–Liouville eigenproblems with interior singularity. *J. Comput. Phys.* **57**, 454–471.

Carton, X. J. & McWilliams, J. C. 1989 Barotropic and baroclinic instabilities of axisymmetric vortices in a quasigeostrophic model. In *Mesoscale/Synoptic Coherent Structures in Geophysical Turbulence* (ed. J. C. J. Nihoul & B. M. Jamart), pp. 225–244. Elsevier.

D'Asaro, E. A. 1988 Observations of small eddies in the Beaufort Sea. *J. Geophys. Res.* C **93**, 6669–6684.

Dewar, W. K. & Killworth, P. D. 1995 On the stability of oceanic rings. *J. Phys. Oceanogr.* **25**, 1467–1487.

Dritschel, D. G. 1988 Nonlinear stability bounds for inviscid, two-dimensional, parallel or circular flows with monotonic vorticity, and the analogous three-dimensional quasi-geostrophic flows. *J. Fluid Mech.* **191**, 575–582.

Helfrich, K. R. & Send, U. 1988 Finite-amplitude evolution of two-layer geostrophic vortices. *J. Fluid Mech.* **197**, 331–348.

Ikeda, M. 1981 Instability and splitting of mesoscale rings using a two-layer quasi-geostrophic model on an f-plane. *J. Phys. Oceanogr.* **11**, 987–998.

Killworth, P. D., Blundell, J. R. & Dewar, W. K. 1997 Primitive equation instability of wide oceanic rings. Part 1: linear theory. *J. Phys. Oceanogr.* **27**, 941–962.

Olson, D. B. 1991 Rings in the ocean. *Annu. Rev. Earth Planet. Sci.* **19**, 283–311.

PALDOR, N. 1999 Linear instability of barotropic submesoscale coherent vortices observed in the ocean. *J. Phys. Oceanogr.* **25**, 1442–1452.

PALDOR, N. & NOF, D. 1990 Linear instability of an anticyclonic vortex in a two-layer ocean. *J. Geophys. Res.* **95**, 18075–18079.

RIPA, P. 1992 Instability of a solid-body rotating vortex in a two-layer model. *J. Fluid Mech.* **242**, 395–417.

TIMOFEEV, A. V. 1970 Oscillation of inhomogeneous flows of plasma and fluid. *Sov. Phys., Uspechi* **13**, 632–646.